J Mater Sci (2007) 42:10180–10187
DOI 10.1007/s10853-007-1983-1

Nucleation behavior and microstructure of Al_2O_3-poor LAS glass–ceramics

K. D. Kim · S. H. Lee · J. H. Hwang · W. S. Seo

Received: 25 April 2006 / Accepted: 9 July 2007 / Published online: 5 September 2007

Abstract Influence of MgO and K_2O on the nucleation behavior of Al_2O_3-poor LAS (Li_2O–Al_2O_3–SiO_2) base glasses was investigated by thermal analysis and, the effect on microstructure and surface topography of glass–ceramics was also examined by SEM, AFM and TEM. According to results of thermal analysis, the exothermic peak temperature of the glass showed a decrease with increase of nucleation temperature to nucleation time of 6 h. But some glasses nucleated for 9 h showed nucleation rate-like curve with maximum point. The dependence of reciprocal value of the exothermic peak temperature on the nucleation temperature indicated that an introduction of MgO might accelerate the nucleation of the base glass and thus result in rough surface topography of glass–ceramics. On the other hand, in the case of glass–ceramics containing K_2O the main crystalline phase was lithium metasilicate and they showed fine microstructure resulting in smooth surface topography. TEM micrographs of as-quenched and nucleated glasses showed no trace of phase separation affecting nucleation or final microstructure.

Introduction

The microstructure of glass–ceramics offers important information for estimating their final properties as well as the surface quality, especially if they are applied to substrate materials in electronic device [1]. The microstructure of glass–ceramics is generally dependent on art, size and amount of existing crystals. Therefore, it has been reported in some patents that it is possible to acquire the optimal surface quality by controlling the microstructure via grain size of some crystal phases [2, 3]. It has been suggested several fundamental parameters affecting the microstructure of glass–ceramics. Thermal history for nucleation or crystal growth, or occurrence of phase separation in the course of crystallization is one of those parameters.

LAS (Li_2O–Al_2O_3–SiO_2) glass–ceramics with low Al_2O_3 content have been expected materials as substrate of information storage device such as computer hard disk drive because of their excellent mechanical strength [4, 5]. Since surface texture of disk substrate is important for determining recording density of hard disk drive, surface roughness value (R_a) of substrate materials should be controlled within the limited range, for example 10–50 Å [4]. According to the previous work [6] in which the effect of MgO and K_2O on surface topography of Al_2O_3-poor LAS glass–ceramics was studied, R_a showed a strong dependence on the microstructure. In the present work, influence of MgO and K_2O on the nucleation behavior of the Al_2O_3-poor LAS glasses was performed by thermal analysis and their effect on microstructure was also investigated. Based on some results it was discussed the compositional dependence of nucleation rate and microstructure.

Experimental procedure

Three different Al_2O_3-poor LAS glass compositions were studied in the present work. The base glass composition

K. D. Kim (✉) · S. H. Lee
Department of Materials Science & Engineering,
Kunsan National University, Kunsan 573-701, Korea
e-mail: kdkim@kunsan.ac.kr

J. H. Hwang · W. S. Seo
Korea Institute of Ceramic Engineering & Technology,
Seoul 153-801, Korea

in mol% was 75.6SiO_2, 20.8Li_2O, 2.7Al_2O_3. 2.8 mol% of SiO_2 in the base glass was replaced by MgO or K_2O. Other minor components as P_2O_5 were introduced additionally to glass batch. Table 1 contains three compositions of the experimental glasses: HDGM (base glass), HDG1 (base glass + MgO) and HDG5 (base glass + K_2O). The raw materials used were reagent grade chemicals. As a fining agent, Sb_2O_3 was used. The batches were mixed thoroughly and melted in a Pt/20Rh crucible with 300cc volume at temperatures between 1500 and 1550 °C in an electric furnace. Sufficient time (2 h) was allowed for the melts to be homogenized by Pt/Rh-stirrer. The bulk glasses were formed on a graphite plate as quenched state. After cooling, they were pulverized or cut in fragment and subsequently treated thermally for the nucleation and crystallization. The glass transition temperatures of HDGM, HDG1 and HDG5 determined by dilatometer were 448, 442 and 448 °C, respectively. According to Phase diagram for LAS system [7] the three melt compositions are positioned in the field of tridymite as primary crystal phase and finally approach to lithium disilicate (Li_2O2SiO_2) with temperature decrease. XRD analysis for glass specimens treated thermally at their liquidus temperatures indicated also Tridymite as an initial crystal phase.

In order to examine the nucleation effect of each glass, thermal analysis technique was utilized. The glass powders of 30 mg with particle size between 425 and 500 μm were used. For nucleation the glass powders had been subjected to various isothermal treatment below 500 °C using a precision horizontal tube furnace with temperature uniformity of ±1 K and then they were subsequently heated up to 1000°C at 10 K/min in DTA cell (TG-DTA 2000, MAC Science, Japan). The first exothermic peak temperatures (T_p) of nucleated glasses were compared with those of as-quenched glasses (T_p^0) and then the relationship between peak temperatures and nucleation state was described.

Transmission Electron Microscope (TEM: JEM-4010, Jeol, Japan) with 400 KV was used to examine the phase separation of as quenched and nucleated glasses. Based on the above results of DTA, the glasses underwent two-step heat treatment and the crystalline phases were identified by X-ray diffraction technique (XRD: M18XCE, Bruker, Germany). The surface topography of some resulting glass–ceramics was examined by Atomic Force Microscopy (AFM: D-300, Digital Instrument, USA). The surface of produced glass–ceramics was polished finely with aid of machine and finished by CeO_2 slurry with 0.05 μm average particle size. Before being examined by AFM, all surfaces were rinsed with acetone to remove surface contamination. All the images of AFM were presented in the area of 10×10 μm^2 in the form of two or three dimension and R_a values were also analyzed. The microstructure analysis was conducted on the same surface using Scanning Electron Microscopy (SEM: JSM-5410, Jeol, Japan). For SEM examination the surface was etched in 2% HF solution for 2 min.

Table 1 Compositions of experimental glasses (in mol% and wt%)

Component	HDGM		HDG1		HDG5	
	Mol%	Wt%	Mol%	Wt%	Mol%	Wt%
SiO_2	75.6	81.3	72.8	79.1	72.8	77
Li_2O	20.8	11.2	20.8	11.3	20.8	11
Al_2O_3	2.7	4.9	2.7	5.0	2.7	4.8
MgO	–	–	2.8	2.0	0	0
K_2O	–	–	0	0	2.8	4.7
P_2O_5	0.8	2.0	0.8	2.1	0.8	2.0
Sb_2O_3	0.1	0.5	0.1	0.5	0.1	0.5

Results

Nucleation behavior traced by DTA

Figure 1 shows a part of DTA curves of three as-quenched glasses which exhibited one or two exothermic peaks due to crystallization. According to XRD analysis as shown in Fig. 2, the first peak was due to crystallization to lithium disilicate (Li_2O2SiO_2:L2S) for HDGM and HDG1, and lithium metasilicate (Li_2OSiO_2:LS) for HDG5. The second peak was due to further phase transition to Quartz as sub-crystal phase for HDG1 and L2S for HDG5. In the case of HDG1, the Quartz peak corresponding to the intensity 100 was detected at 26.3 degree

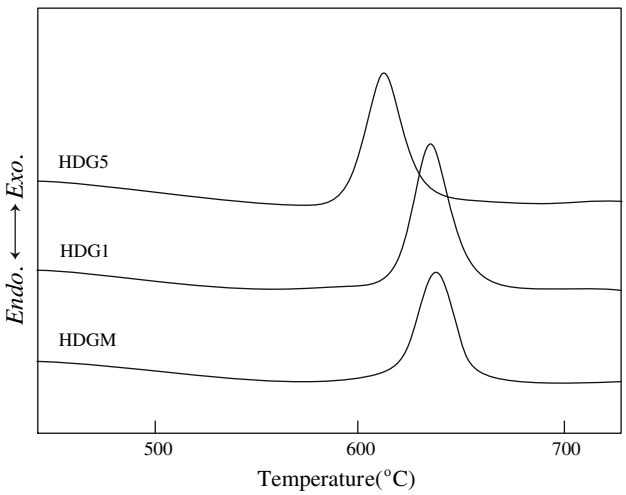

Fig. 1 DTA curves of three as-quenched glasses. HDGM: base glass, HDG1: base glass + MgO, HDG5: base glass + K_2O

by XRD. DTA curves for HDGM nucleated at various temperatures for 9 h are shown in Fig. 3. The first peak temperature (T_p) is shifted to lower temperature with increase of nucleation temperature. HDG1 and HDG5 showed the same dependence of DTA trace on nucleation temperature. In Fig. 4a–c T_p for three glasses at various nucleation times is plotted as function of the nucleation temperature in the range of 400–500 °C. The peak temperature (T_p^0) of the as-quenched glasses is 638 °C for HDGM, 636 °C for HDG1 and 612 °C for HDG5. T_p decreases slightly at initial nucleation temperature of about 440 °C irrespective of nucleation time. But, passing through this nucleation temperature, T_p of glasses nucleated more than 3 h begins to decrease drastically. In the case of (b) HGD1 and (c) HGD5 in Fig. 4, minima are clearly shown when the nucleation time was 9 h. In all specimens nucleated at 500 °C for 9 h, trace of peaks due to crystallization was detected by X-ray diffraction analysis as shown in Fig. 5.

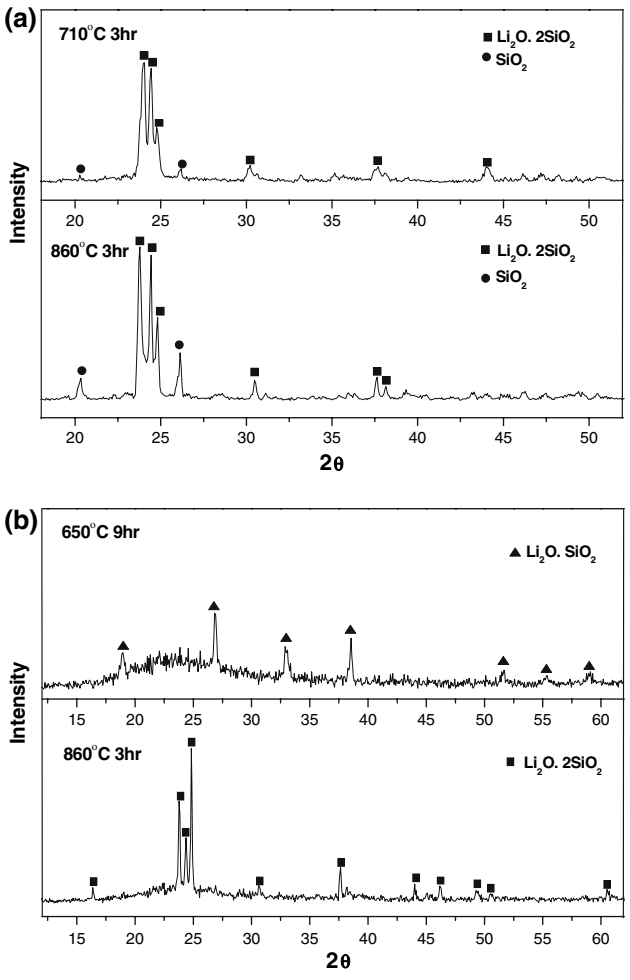

Fig. 2 XRD patterns and identified phases for (**a**) HDG1 (base glass + MgO) and (**b**) HDG5 (base glass + K_2O) with denotation of heat treatment condition

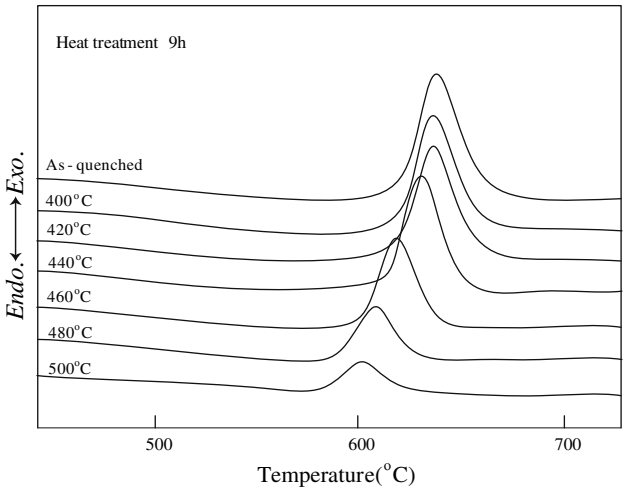

Fig. 3 DTA curves of HDGM (base glass) nucleated at various temperatures for 9 h

Micrograph examined by TEM

Phase separation was not observed according to the transmission electron micrographs for all as-quenched glass specimens. Figure 6 shows TEM images of HDG1 and HDG5 glasses nucleated at 460 °C for 9 h. No phase separation was also observed in these glasses. However, as shown in TEM image of Fig. 7 the glasses nucleated at 500 °C for 9 h indicate a different micrograph in nanometer range from those of Fig. 6 because they were slightly crystallized as confirmed by XRD of Fig. 5. Figure 7a and b show a similar micrograph with independent spheres of about 20–30 nm in the glass matrix. On the other hand, crystal phase occurring in HDG5 of Fig. 7c is interconnected and thus its micrograph is different from those of both glasses. Therefore, it can be expected also a microstructure difference between HDG1 and HDG5 in glass–ceramics produced by subsequent heat treatment.

Microstructure by SEM and surface topography by AFM

Figure 8 illustrates SEM images for HDGM (a, b) and HDG1 (c, d) glass–ceramics with different nucleation history. Specimen (a) and (c) were nucleated at 420 °C for 6 h, and then heated at 680 °C for 6 h. Specimens (b) and (d) were nucleated at 480 °C for 6 h and then heated at the same condition. After heat treatment, the HDGM specimens were opaque but seemed to contain relatively high amount of glass phase by visual check. The microstructure of HDGM is hence simple due to high concentration of glass phase in spite of containing L2S as crystalline phase. HDGM (b) shows quasi dendrite form. But there exists a distinct difference between (a) and (b) in their

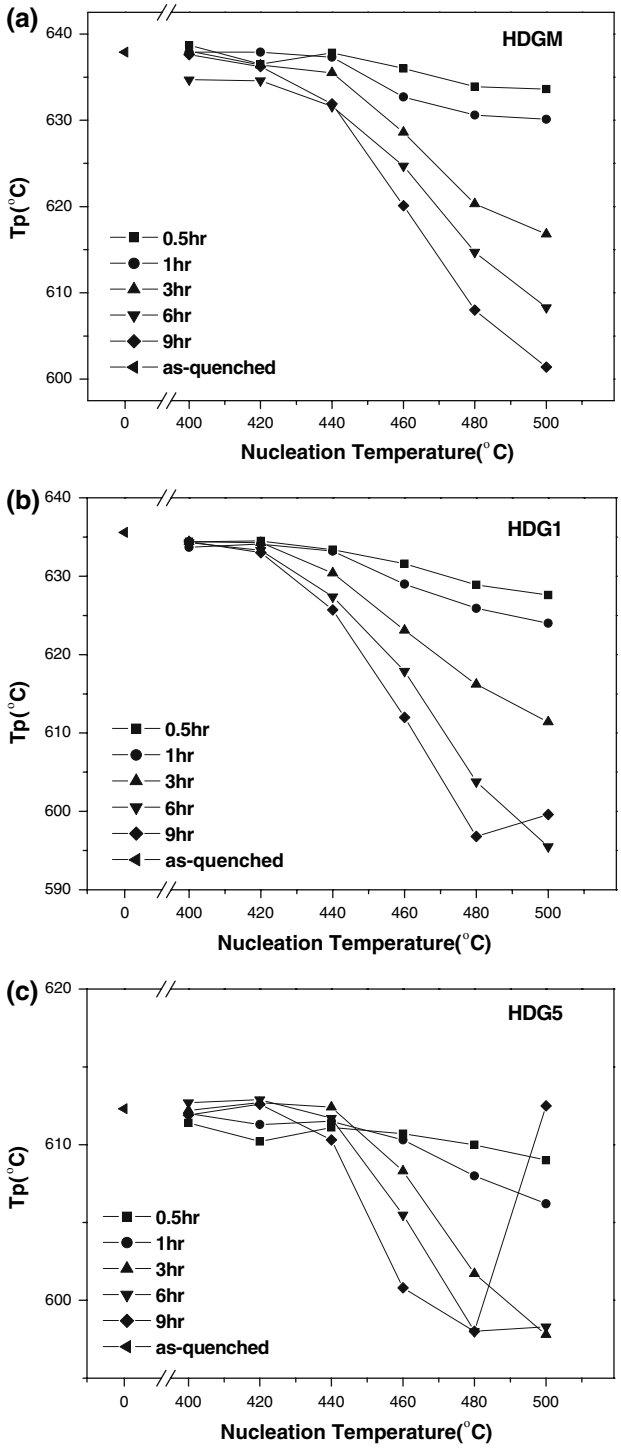

Fig. 4 T_p as function of the nucleation temperature for three glasses. DGM: base glass, HDG1: base glass + MgO, HDG5: base glass + K_2O

microstructure. In the case of HDG1, unlike HDGM it shows a clear dendrite and the microstructure of specimen (d) nucleated at 480 °C is finer than that of specimen (c) nucleated at 420 °C as shown in Fig. 8.

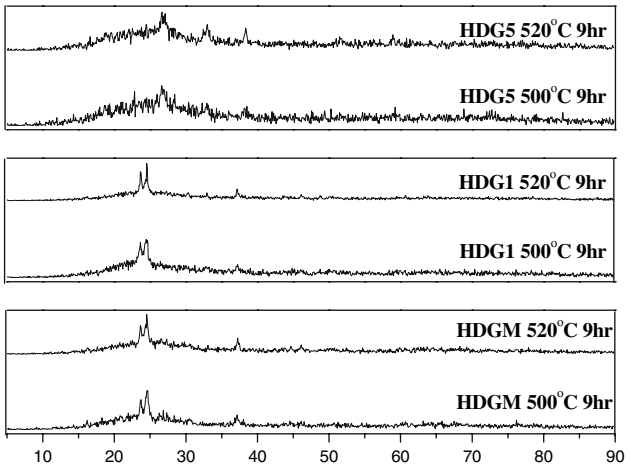

Fig. 5 XRD pattern of three glasses nucleated for 9 h at 500 and 520 °C HDGM: base glass, HDG1: base glass + MgO, HDG5: base glass + K_2O

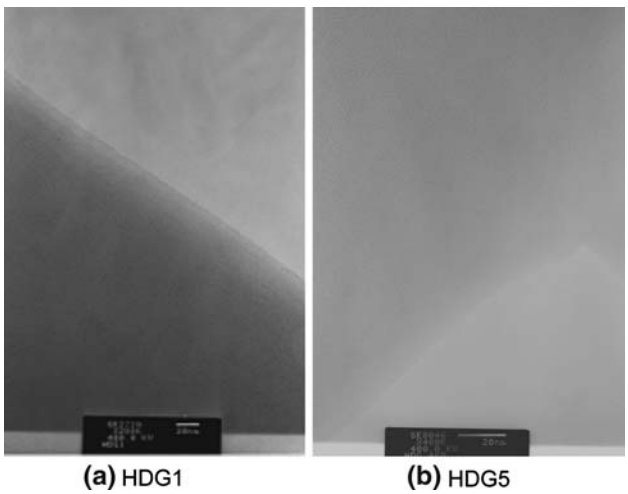

Fig. 6 TEM images of nucleated glasses at 460 °C for 9 h showing absence of phase separation. The bar denotes 20 nm. HDG1 (base glass + MgO), HDG5 (base glass + K_2O)

Figure 9 presents AFM images of HDGM and HDG1 corresponding to specimens (b) and (d) of Fig. 8. The surface of HDGM within area of 10×10 μm^2 examined by AFM appears to be smooth and plane. Its R_a value is as low as that of polished glass surface because of high amount of glass phase. However, R_a value of HDG1 glass–ceramics lies in 30Å approximately. Its pseudo-three-dimensional image indicates many broad valleys corresponding to the surface texture shown in SEM micrograph of Fig. 8d.

Figure 10 exhibits SEM and AFM images of HDG5 specimen crystallized at 680 °C for 6 h after nucleation for 6 h at 420 °C and 480 °C, respectively. The main crystal phase of HDG5 glass–ceramics is LS and thus the

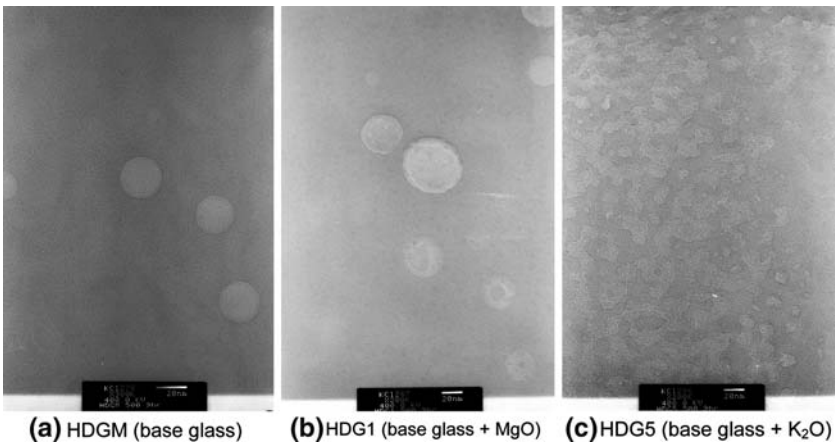

Fig. 7 TEM images of nucleated glasses at 500 °C for 9 h showing independent spheres (**a**), (**b**) and interconnected phase (**c**). The bar denotes 20 nm

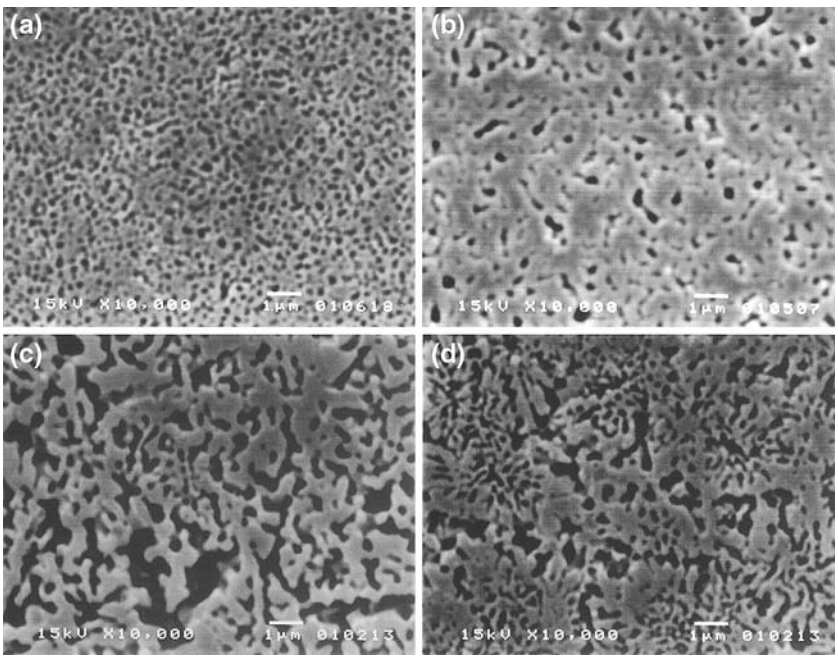

Fig. 8 SEM images for HDGM (**a**, **b**) and HDG1 (**c**, **d**) glass–ceramics with different nucleation history. The bar denotes 1 μm. HDGM: base glass, HDG1: base glass + MgO

morphology is different from that of HDG1 in Fig. 8. Such difference was already expected from TEM micrograph of Fig. 7. There exists also slight difference in morphology between two specimens (a) and (b) in Fig. 10 due to different nucleation history. The specimen (a) shows a loose microstructure in which small and large crystals are mixed. On the other hand, the specimen (b) has a fine microstructure composed of crystals with relatively uniform size. The surface of glass–ceramics nucleated at high temperature is hence smoother than that of low temperature. In the case of those nucleated at 480 °C, R_a lay in the range of 11–22 Å. Comparing AFM images of specimen (b) in Fig. 10 with that of HDG1 in Fig. 9, narrower valleys and lower peaks are observed in HDG5 glass–ceramics and thus its R_a is much lower than that of HDG1.

Discussion

Recently, several studies performed by DTA [8–10] reported that the exothermic peak temperature (T_p) due to crystallization was important to understand the nucleation behavior of a glass. Since the crystallization peak temperature in DTA curve depends on nucleation treatment of glass, the shift of T_p plays a role of indicator showing the influence of nucleation state indirectly. Based on the dependence of $\left((1/T_P) - (1/T_P^0)\right)$ or $1/T_P$ on the nucleation temperature of glass, a nucleation rate-like curve (NRC) with maximum point could be yielded [8, 11, 12], and those results by DTA technique were confirmed by kinetic studies performed by microscopy method [11, 13, 14]. In those studies it was indicated that temperature and time for nucleation is related with crystal nucleation

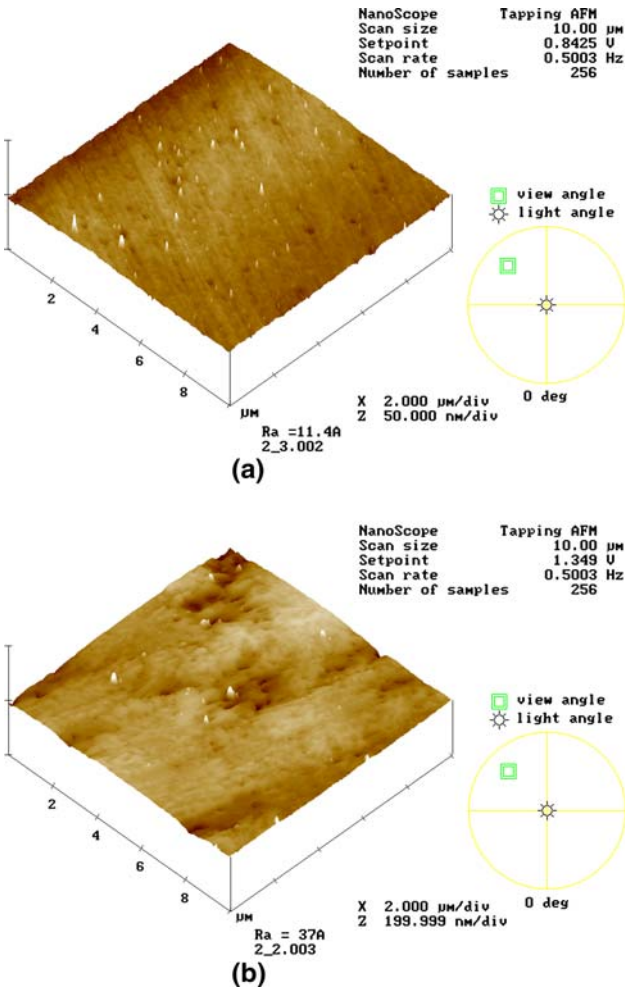

Fig. 9 AFM images of HDGM and HDG1 glass–ceramics nucleated at 480 °C for 6 h, and then heated at 680 °C for 6 h. HDGM: base glass, HDG1: base glass + MgO

density inducing the shift of T_p. In the present work, the dependence of $\left((1/T_P) - (1/T_P^0)\right)$ on nucleation temperature and time was also observed and its temperature dependence is presented in Fig. 11 for glasses nucleated for 6 and 9 h. Since some minima were found in the plot of T_p versus nucleation temperature of Fig. 4, NRC can be yielded for HDG1 and HDG5 nucleated for 9 h shown in Fig. 11b. It is expected theoretically that the maximum point is shifted to lower nucleation temperature when the nucleation time is more than 9 h [15]. In relation to the compositional dependence of nucleation effect it is very interesting the work of Heslin et al. [14] in which the influence of water on nucleation effect in Li_2O–SiO_2 glasses was performed qualitatively by DSC and quantitatively by microscopy. In that work both results indicated the same trends in NRC and thus the approach via thermal analysis technique seems to be reliable within a limited range in comparing a compositional dependence of nucleation effect relatively. Therefore, based on the results of $\left((1/T_P) - (1/T_P^0)\right)$ versus nucleation temperature for three glasses in Fig. 11 it can be supposed that the nucleation kinetics of the base glass (HDGM) is accelerated with introduction of MgO and decelerated with K_2O, respectively. However, in the case of K_2O the relative comparison is unreasonable because the resulting crystalline phase is different. The nucleation effect by introduction of MgO will be discussed in conjunction with microstructure of glass–ceramics.

The nucleation improvement by introduction of MgO as discussed above is revealed clearly by difference of spherical crystal density between (a) HDGM and (b) HDG1 nucleated at 500 °C for 9 h as shown in TEM micrographs of Fig. 7. In general, higher nucleation density results in finer microstructure [16]. The SEM micrographs of two specimens in Fig. 8 that were nucleated and followed by heat treatment to accomplish crystal growth indicate a better-developed microstructure for glass containing MgO (HDG1) than HDGM. The microstructure of HDG1 shows distinct morphology as dendrite although both glass–ceramics contains the same crystalline phase (L2S) under the same thermal program. However, due to the existence of the large dendrite-typed crystals with deep valley and high peak, the R_a value of HDG1 glass–ceramics is high relatively as shown in Fig. 9. In the case of HDG5 glass–ceramics, the crystal morphology in microstructure is fundamentally different from that of HDG1 because they contain LS as crystalline phase. The size of crystal is less than 1 µm and there is a little difference in their distribution depending on nucleation state as shown in Fig. 10. The corresponding pseudo-three-dimensional AFM images reflect such microstructure.

In relation to the role of phase separation on the course of crystallization, many works have been carried out for a long time [17–19]. Even though there is still a discrepancy one another it seems to be major opinion that phase separation is not inevitable to generate crystal nucleation or growth in glass. However, if phase separation occurs its influences on the crystallization cannot be excluded. Hence, the occurrence of phase separation would also affect nucleation and final microstructure of glass–ceramics that depends on morphology and distribution of precipitated crystal. It is well known that L_2O–SiO_2 glasses containing less than 33 mol% Li_2O show a strong tendency to phase separation [20, 21]. It was also observed in L_2O–Al_2O_3–SiO_2 glasses depending on Al_2O_3 concentration [22–24] and thus present glasses containing minor component such as MgO or K_2O could have also high possibility for phase separation. Therefore, it was attempted an approach to phase separation for present glasses in order to examine its eventual influence on nucleation and microstructure. According to TEM micrographs, however, phase separation did not occur in both as-quenched and

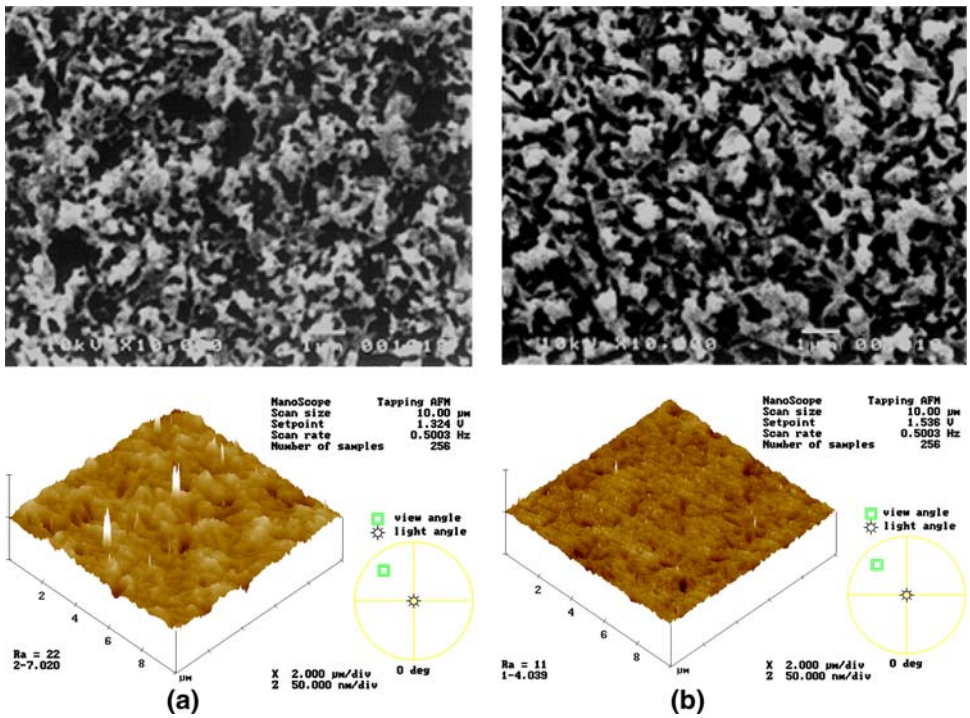

Fig. 10 SEM (upper) and AFM (lower) images of HDG5 (base glass + K_2O) glass–ceramics nucleated for 6 h at (**a**) 420 °C and (**b**) 480 °C, The bar in SEM denotes 1 μm

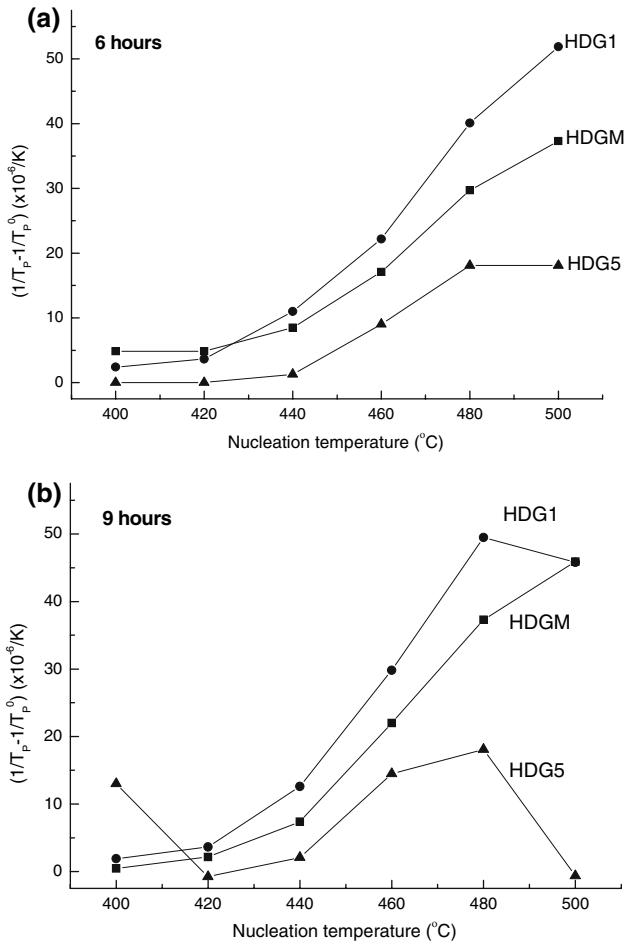

◀ **Fig. 11** Dependence of $\left((1/T_P) - (1/T_P^0)\right)$ on nucleation temperature for three glasses nucleated for (**a**) 6 h (**b**) 9 h HDGM: base glass, HDG1: base glass + MgO, HDG5: base glass + K_2O

nucleated glasses. It could be found only the influence of MgO and K_2O on crystal morphology of nucleated glasses as shown in Fig. 7.

Conclusion

In the present work the influence of MgO and K_2O on the nucleation behavior and phase separation of the Al_2O_3-poor LAS base glasses was investigated. Microstructure and surface topography for the corresponding glass–ceramics was also studied.

The exothermic peak temperature (T_p) of glass determined by DTA decreased depending on nucleation temperature (400–500 °C) and time (0.5–6 h). However, nucleation rate-like curve (NRC) with maximum point in $\left((1/T_P) - (1/T_P^0)\right)$ versus nucleation temperature was found only for some glasses with long nucleation time (9 h). According to its compositional dependence MgO might improve the nucleation of the base glass what was proved by TEM and SEM micrographs of glass–ceramics containing lithium disilicate. In the case of glass–ceramics containing K_2O, since the existing crystalline phase was lithium metasilicate their microstructure was fine unlike that of MgO. The topography of the corresponding surface examined by AFM reflected such microstructure. No trace

of phase separation shown in TEM micrographs of as-quenched and nucleated glasses indicated that nucleation or microstructure investigated in the present work was free from phase separation.

Acknowledgements A part of this work was performed in Fraunhofer Insitut Silicatforschung (ISC), Wuerzburg, Germany. The corresponding author acknowledges for the kind help of Prof. Dr. G. Mueller, Dr. B. Durschang and Dr. M. Krauss in ISC, and thanks Korea Research Foundation Grant (KRF 2003–013-D00056) for the financial support during stay in ISC.

References

1. Lewis MH (1989) In: Glasses and glass–ceramics. Chapman and Hall p 226
2. Goto N, Yamaguchi K (1996) USA-pat. no. 5567217. Filed date May. 16, 1995, issued date Oct. 22, 1996
3. Yamaguchi K (1999) USA-pat. no. 5985777. Filed date Sep. 10, 1998, issued date Nov. 16, 1999
4. Goto N (1995) New Glass 10(4):56
5. Pannhorst W (2000) Glastech Ber Glass Sci Technol 73C1:28
6. Kim KD, Kim YJ, Hwang JH (2002) Glass Technol 43C:202
7. Levin EM, Robbins CR, McMurdie HF (1985) In: Phase diagrams for ceramists. The American Ceramic Society, p 118
8. Xu XJ, Ray CS, Day DE (1991) J Am Ceram Soc 74:909
9. Ray CS, Day DE (1997) J Am Ceram Soc 80:3100
10. Kim KD, Lee SH, Ahn HK (2004) J Non-Cryst Solids 336:195
11. Burgner LL, Weinberg MC (2000) J Non-Cryst Solids 261:161
12. Marotta A, Buri A, Branda F, Saiello S (1982) In: Advance in ceramics: Vol. 4. Nucleation and crystallization in glasses. American Ceramic Society, Columbus, OH, p 146
13. Wakasugi T, Burgner LL, Weinberg MC (1999) J Non-Cryst Solids 244:63
14. Heslin MR, Shelby JE (1992) In: Weinberg MC (ed) Ceramic transactions: Vol. 30. Nucleation and crystallization in liquids and glasses American Ceramic Society, Columbus, OH, p 189
15. Frade JR, Queiroz CM, Fernandes MH (2004) J Non-Cryst Solids 333:263
16. McMillan PW (1979) In: glass–ceramics. Academic Press, p 100
17. Zanotto ED, James PF (1983) In: Proceedings of the 13th Int. Congress on Glass, Hamburg published by Verlag der DGG, p. 794
18. Ramsden AH, James PF (1984) J Mat Sci 19:1406
19. Ramsden AH, James PF (1984) J Mat Sci 19:2894
20. Moriya Y, Warrington DH, Douglas RW (1967) Physics Chem Glasses 8:19
21. Haller W, Blackburn DH, Simmons JH (1974) J Am Ceram Soc 57:120
22. Barry TJ, Lay LA, Miller RP (1970) Discuss Farad Soc 50:214
23. Nakagawa K, Izumitani T (1972) Physics Chem Glasses 3:85
24. Kawamoto Y (1985) J Mat Sci 20:2695